

## Limits on Fluorescence Detected Circular Dichroism of Single Helicene Molecules

Yiqiao Tang,<sup>†</sup> Timothy A. Cook,<sup>‡,§</sup> and Adam E. Cohen\*,<sup>†,‡</sup>

Department of Physics, Harvard University, Cambridge, Massachusetts 02138, and Department of Chemistry and Chemical Biology, Harvard University, Cambridge, Massachusetts 02138

Received: April 19, 2009; Revised Manuscript Received: May 6, 2009

Fluorescent imaging of single helicene molecules is applied to study the optical activity of chiral fluorophores. In contrast to the previous report by Hassey et al. (*Science* **2006**, *314*, 1437), the dissymmetry factors of single chiral fluorophores are found not to differ significantly from the bulk value of  $|g| < 10^{-4}$  at 457 nm. Linear dichroism and birefringence of the dichroic mirror inside the fluorescence microscope change the polarization state of the incoming laser beam significantly; i.e., circular polarized light sent into the microscope becomes highly elliptically polarized after reflection from the dichroic mirror. Compensation for this effect should be made to avoid artifacts brought by linear dichroism in single immobilized molecules.

Single-molecule measurements have been used to probe the states and dynamics of a huge variety of biophysical and condensed matter systems,<sup>2–4</sup> and often yield information that is missed by bulk, ensemble-averaged techniques. In particular, measurements at ambient and low temperatures provide detailed information about the interactions between single fluorescent molecules and their local environment. The heterogeneously broadened lines visible in bulk often resolve into much narrower single-molecule lines, which show spectral diffusion,<sup>5,6</sup> blinking,<sup>7</sup> and polarization fluctuations<sup>8,9</sup> that indicate complex interactions with the host.

Chiral molecules of a single enantiomer show differential absorption of left and right circularly polarized light (CPL). The degree of circular dichroism (CD) at a particular frequency is measured by the *g*-value:

$$g \equiv \frac{2(\Gamma^+ - \Gamma^-)}{(\Gamma^+ + \Gamma^-)}$$

where  $\Gamma^\pm$  is the rate of excitation in right (+) or left (-) CPL. The *g*-value varies between  $-2 \leq g \leq 2$ . For most small organic molecules, peptides, nucleic acids, and sugars,  $|g| < 10^{-3}$  in the visible.<sup>10</sup> The smallness of *g* arises from the small size of molecules relative to the helical pitch of CPL: the electromagnetic field undergoes a nearly imperceptible twist over a distance of molecular dimensions.

At the quantum mechanical level, CD arises through an interference between electric dipole and either electric quadrupole or magnetic dipole transitions.<sup>11</sup> The Hamiltonian relevant to CD for a chiral molecule in an electromagnetic field is:<sup>12–14</sup>

\* To whom correspondence should be addressed. E-mail: cohen@chemistry.harvard.edu.

<sup>†</sup> Department of Physics.

<sup>‡</sup> Department of Chemistry and Chemical Biology.

<sup>§</sup> Current address: School of Law, University of Virginia, Charlottesville, VA 22903.

$$H = -\mu \cdot \mathbf{E} - \boldsymbol{\theta} : \nabla \mathbf{E} - \mathbf{m} \cdot \mathbf{B}$$

where  $\mu$  is the electric dipole operator,  $\boldsymbol{\theta}$  is the electric quadrupole operator, and  $\mathbf{m}$  is the magnetic dipole operator;  $\mathbf{E}$  is the electric field, and  $\mathbf{B}$  is the magnetic field. The rate of excitation from an initial state *i* to a final state *f* involves the expression  $\langle f | H | i \rangle^2$ , as specified by Fermi's golden rule. This expression contains a term proportional to  $|\mu_{if}|^2$ , as well as cross-terms containing  $\mu$  and  $\boldsymbol{\theta}$  or  $\mu$  and  $\mathbf{m}$  (the remaining terms are small enough to be neglected). The term containing  $|\mu_{if}|^2$  represents electric dipole absorption, and is not sensitive to molecular chirality. The signs of the two cross-terms, however, depend on molecular chirality, so these terms are responsible for circular dichroism. Both cross-terms depend on the orientation of the molecule relative to the incident field. Upon averaging over all molecular orientations, the electric quadrupole contribution to the differential absorption averages to zero while the magnetic dipole term remains.<sup>13</sup> Thus, electric quadrupole transitions do not contribute to bulk CD, while magnetic dipole transitions do contribute.

In light of the increased information available from single-molecule measurements, it is interesting to compare the chiroptical response of a single chiral molecule to the ensemble-averaged response. One can measure chiroptical effects in small samples by using fluorescent chiral molecules.<sup>15,16</sup> The rate of fluorescence emission is proportional to the rate of excitation, and thus, fluorescence detected circular dichroism (FDCD) provides a possible probe of chiroptical effects at the single-molecule level. Single-molecule FDCD might differ from bulk FDCD for several reasons:

(1) Electric quadrupole and magnetic dipole matrix elements of orientationally fixed single molecules may differ from their rotationally averaged values in bulk systems.<sup>13,17</sup>

(2) Local interactions with the host could modify the oscillator strengths or frequencies of the electric quadrupole or magnetic dipole transitions, to induce molecule-to-molecule variations in CD, i.e., heterogeneous broadening of CD lines.

The smallness of the electric quadrupole and magnetic dipole contributions to the Hamiltonian is purely geometrical in origin,

a consequence of the small size of a molecule relative to the wavelength of light. Orientational averaging reduces the strength of the electric dipole/magnetic dipole interference by a factor of 3 relative to its peak value.<sup>13</sup> Electric quadrupole transitions average to zero in bulk, so bulk measurements provide no guidance on their magnitude. Geometrical considerations, however, indicate that the electric quadrupole term should be of the same order of magnitude as the magnetic dipole term. Density functional simulations of single helicene molecules support the prediction that single-molecule *g*-values are of the order of  $10^{-3}$ , of the same order as in bulk at the same excitation wavelength.<sup>18</sup>

Nonetheless, theoretical models may be wrong, so there was considerable interest in the report from Hassey et al.<sup>1</sup> that single molecules of bridged triarylamine helicenes show *g*-values ranging from +2 to -2, while in bulk the two enantiomers have  $|g| < 10^{-4}$  at a probe wavelength of 457 nm. Furthermore, they reported that both enantiomers of this compound show very similar broad distributions of single-molecule *g*-values, and that the wavelength dependence of the single-molecule *g*-values does not correspond to the bulk, even when averaged over many single molecules.<sup>18</sup>

We attempted to replicate the experiments of Hassey et al. and initially saw similar broad distributions of *g*-values. However, after correcting for the linear birefringence and linear dichroism inherent to the dichroic mirrors used in single-molecule FDOD experiments, the distribution of *g*-values collapses to a sharp distribution around *g* = 0. The uncertainty in the measurements does not allow us to distinguish the *g*-values of opposite enantiomers.

## Methods

Triarylamine helicenes M-2 and P-2 (Figure 1a) were synthesized following literature procedures<sup>19,20</sup> with modifications. (2-Methoxyphenyl)-naphthalenylamine was synthesized using (1,1'-bis(diphenylphosphino)ferrocene)PdCl<sub>2</sub>·CH<sub>2</sub>Cl<sub>2</sub> as the amination catalyst,<sup>21</sup> and deprotection of the helicene methyl ether was accomplished using BBr<sub>3</sub>.<sup>22</sup> The molecules we prepared are identical to the ones Hassey et al. used in ref 1.

The products were characterized by <sup>1</sup>H NMR, <sup>13</sup>C NMR, and mass spectrometry; all data match the literature spectra. The circular dichroism (Figure 1b) and fluorescence (not shown) spectra are identical to earlier reports.<sup>19</sup> Both enantiomers show strong FDOD in bulk when excited with light at 355 nm, with *g*-values of  $+8.0 \times 10^{-3}$  for M-2 and  $-8.1 \times 10^{-3}$  for P-2. At 457 nm, the wavelength used in the experiments of Hassey et al., the *g*-values are  $|g| < 10^{-4}$ .

Following the procedure of Hassey et al., we made solutions of the helicenes at  $10^{-8}$  M in methanol and drop-cast these solutions onto a Zeonor film (ZF-14 ZEONEX/ZEONOR). A fused silica coverslip was cleaned in Piranha solution (3:1 H<sub>2</sub>SO<sub>4</sub>:H<sub>2</sub>O<sub>2</sub>, *Caution*: highly corrosive). The Zeonor film was placed, helicene side down, onto the coverslip, and the samples were imaged in an inverted single-molecule fluorescence microscope.

The optical setup is shown in Figure 2a. The setup is built around an Olympus IX71 inverted fluorescence microscope. The light source is a Melles Griot argon-ion laser operating at 457 nm (0.4 mW at the sample). A narrow-band excitation filter (D457/10x Chroma) is used to remove plasma emission at other wavelengths. The light is polarized by a Glan Thompson polarizer (10GL08 Newport), passed through a liquid crystal variable retarder (LCVR, LRC - 200 - VIS, Meadowlark Optics), and then through a quarter wave Fresnel rhomb retarder

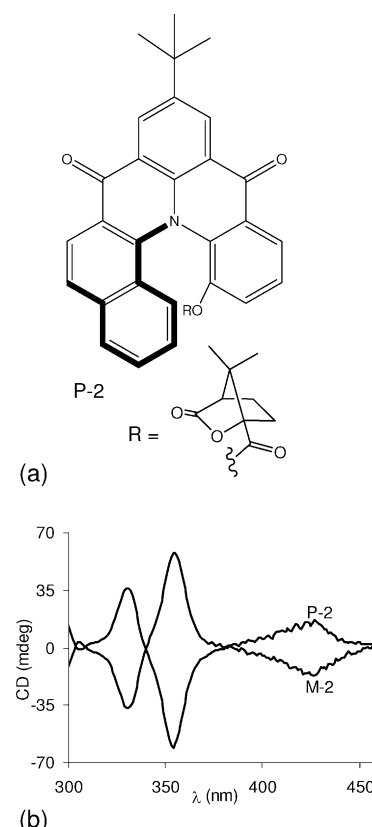


**Figure 1.** Bridged triarylamine helicenes. (a) Structure of the P-2 enantiomer. The camphanate group is used as a chiral resolving agent and renders the M-2 and P-2 species technically diastereomers. However, the camphanate group has no detectable effect on the optical properties of either species. (b) Circular dichroism spectrum of M-2 and P-2, measured with a JASCO CD spectrometer. The spectrum of the P-2 was scaled by a constant factor to correct for a slight difference in concentration between the two samples.

(FM600QM Thorlabs). The LCVR is driven with a 2 kHz square wave. An arbitrary state of ellipticity is generated by adjusting the LCVR drive voltage. We have mirrors between the polarizer and the microscope, to avoid introducing spurious phase shifts onto the beam. The only reflection after the initial polarizer is off the dichroic mirror.

A lens with a focal length of 15 cm (LA1433-A Thorlabs) brings the light to a focus at the back focal plane of the objective. After passing through the lens, the light is deflected upward by a dichroic mirror. We performed experiments using either of two dichroics: DC1, 460 nm long pass; DC2 (Olympus DM500), 500 nm long pass. Our objective lens is a 60×, N.A. 1.45, oil immersion, plan apochromat (1-U2B616 Olympus). Fluorescence from the sample is collected by the same objective, passed through the dichroic mirror, and separated from the excitation light by a 470 nm long-pass emission filter (HQ470LP Chroma). Images are collected on an Andor iXon<sup>+</sup> electron-multiplying CCD (DU-897E-CS0-#BV), cooled to -50 °C.

A program written in LabView synchronizes the acquisition of images with the application of voltages to the LCVR. The LCVR has an ~30 ms response time to a change in the amplitude of its driving voltage, so each image acquisition starts 100 ms after a change in the voltage on the LCVR. In a typical experiment, 40 images are acquired, at 400 ms exposure per frame, with a switch in the polarization state between each frame. An amplified photodiode detector (PDA36A, Thorlabs) is mounted on top of the microscope to monitor the intensity

of the transmitted laser beam. This photodetector allows us to correct for laser power fluctuations.

Prior to each experiment, we measure the polarization state of the light entering the microscope and emerging from the objective. A polarizer (GL10 Thorlabs) is temporarily placed in the beam path at the point of measurement. The transmitted intensity is recorded using a power meter (FieldMaxII-T0 Coherent Inc.) as a function of the angle of the polarizer.

Data are acquired under two conditions for each enantiomer: alternating left- and right-CPL sent into the microscope and alternating left- and right-CPL at the sample plane. The analysis for all movies is completely automated using custom software written in Matlab, with identical parameters for all data sets. Thus, there is no possibility for bias in selecting molecules or extracting their intensities.

## Results

Figure 2b shows an image of single helicene molecules on the Zeonor film. We first imaged the molecules with alternating left- and right-CPL sent into the microscope. For both polarizations, the ellipticity before the microscope is greater than 96%. Many molecules show strong asymmetries in their brightness, as shown in Figure 3b, leading to apparent  $g$ -values ranging from  $-2$  to  $2$ . However, under these conditions the light emerging from the microscope is not circularly polarized. Ellipticities are 36% for DC1 and 55% for DC2.

To generate CPL at the sample, we measured the Jones matrices<sup>23</sup> for the dichroics. They are

$$\begin{pmatrix} 1 & 0 \\ 0 & 1.34e^{0.79i} \end{pmatrix}$$

and

$$\begin{pmatrix} 1 & 0 \\ 0 & 0.97e^{0.39i} \end{pmatrix}$$

for DC1 and DC2, respectively. We solved the matrix equations to identify the Jones vectors of the input polarization states which lead to CPL at the sample. These are

$$\frac{1}{1.25} \begin{pmatrix} 1 \\ \pm 0.75e^{0.78i} \end{pmatrix}$$

for DC1 and

$$\frac{1}{1.43} \begin{pmatrix} 1 \\ \pm 1.03e^{1.18i} \end{pmatrix}$$

for DC2. These polarizations are generated by applying appropriate voltages to the LCVR. Measurements confirmed ellipticities  $>96\%$  above the sample for both right- and left-CPL.

Figure 3b shows a histogram of  $g$ -values measured for single molecules with CPL before the microscope (using DC1) and with CPL at the sample (using DC2). The apparent  $g$ -values are broadly distributed in the case where the CPL is generated before the microscope, using either DC2 (data not shown) or DC1. In contrast, with CPL at the sample, the  $g$ -values are not significantly different from zero:  $g = 0.026 \pm 0.27$  for M-2 and  $g = 0.033 \pm 0.29$  for P-2. The width of the observed distribution is largely due to statistical uncertainties in the extraction of single-molecule  $g$ -values in the presence of shot-noise and molecular blinking and photobleaching. Thus, current experimental techniques cannot detect deviations from 0 in the  $g$ -values of single helicene molecules measured at 457 nm.

## Discussion

We have shown that the broad distribution of  $g$ -values observed by Hassey et al. can be explained by *linear dichroism*<sup>24</sup> in the randomly oriented helicene molecules, coupled with imperfect circular polarization of the illumination. We believe that such a mechanism is a more probable explanation for their data than is anomalously large circular dichroism at the single-molecule level, which would require a hitherto unknown physical effect. In addition to the dichroic mirrors discussed above, a third dichroic mirror with a cutoff of 570 nm (Olympus DM570) also shows strong linear birefringence for 532 nm light. We conclude that strong linear birefringence is a general feature of dichroic mirrors. Finding a dichroic with nearly equal

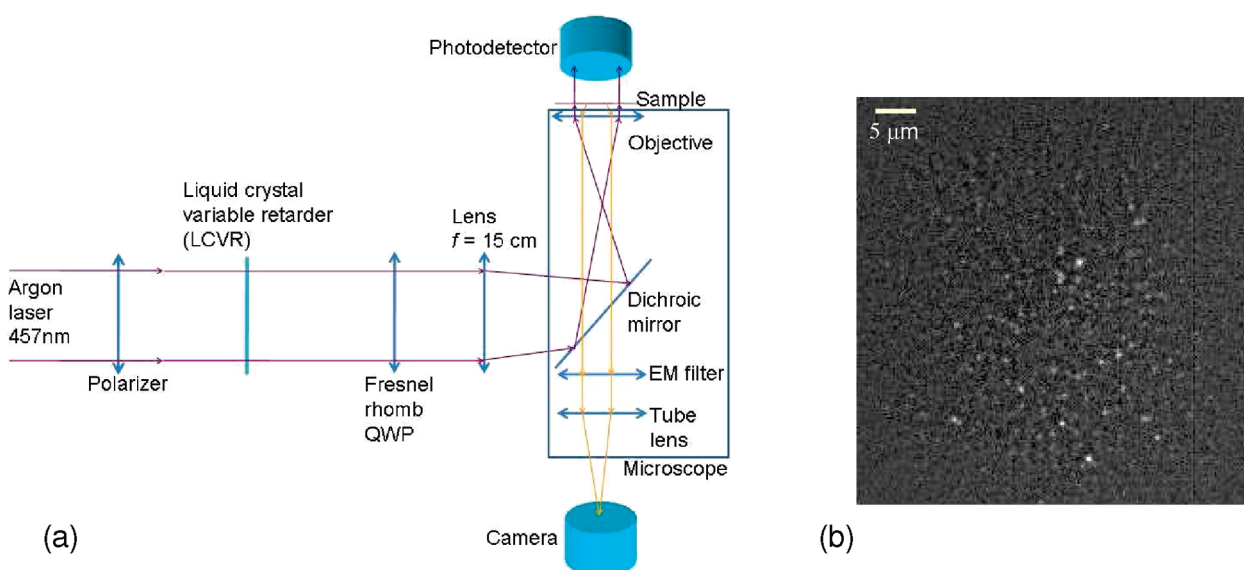


**Figure 2.** Imaging of single helicene molecules under light of controlled polarization. (a) Schematic diagram of optical setup for wide-field imaging. See text for a detailed description. (b) Image of single helicene molecules. A diffuse background image, calculated using a 2-dimensional median filter, was subtracted from the raw image to enhance the contrast of the single molecules.

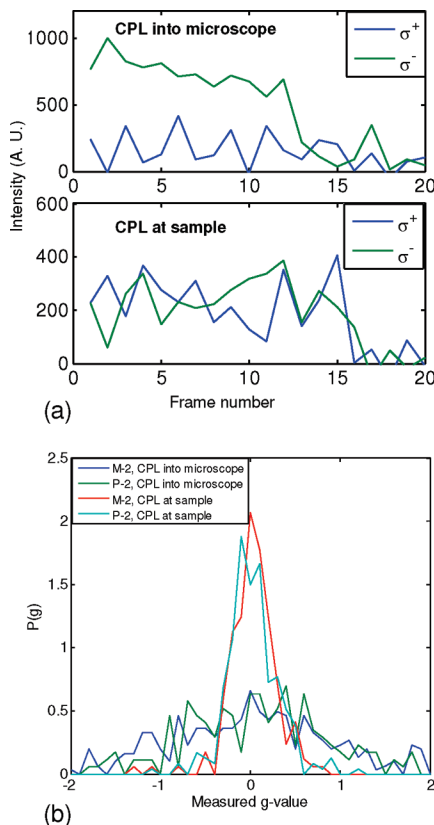


**Figure 3.** Fluorescence of single helicene molecules in CPL. (a) Time-traces of single helicene molecules with CPL sent into the microscope (top) and CPL generated at the sample plane (bottom). There is a large apparent *g*-value when CPL is sent into the microscope but not when CPL is generated at the sample. Both molecules show single-step photobleaching. (b) Histogram of *g*-values for both enantiomers, under both polarization conditions. With CPL at the sample, the *g*-values are much more narrowly distributed. The number of molecules measured for each histogram are the following: M-2 CPL in, 303; P-2 CPL in, 173; M-2 CPL out, 169; P-2 CPL out, 234.

reflectivities for *s*- and *p*-polarized light (such as our dichroic DC2) is not sufficient to preserve the polarization state of incident light; the phase shift between *s*- and *p*-polarizations is important too. An observation of CPL in light back-reflected from the sample is also not proof of CPL at the sample, because the back-reflected light has undergone a second phase-shifting reflection at the dichroic.

If CPL is sent into a fluorescence microscope, the dichroic mirror converts this light into elliptically polarized light at the sample, with different principal axes arising from the two input circular polarizations. The linearly polarized component of this illumination leads to different rates of pure electric dipole excitation for each randomly oriented molecule. Many authors have documented the perils of performing microscopic CD measurements.<sup>14,23,25</sup> Claborn and co-workers avoided any

reflective elements in their optical train and so were not subject to this source of error.<sup>25</sup>

Circular dichroism measurements at the single-molecule level promise important information on molecular structure and local environmental interactions. However, uncompensated linear birefringence and linear dichroism in optical elements inside a microscope can cause linear dichroism to masquerade as circular dichroism. Caution is advised in performing and interpreting such experiments.

**Acknowledgment.** We thank Prashant Jain and Sijia Lu for helpful discussions, Charles Lieber and Sunney Xie for loans of equipment, and Gregory Verdine for use of the CD spectrometer. We thank Michael Barnes for comments on an early draft of this manuscript. This work was partially supported by a Dreyfus New Faculty Award and the MITRE Corporation and the U.S. Government's Nano-Enabled Technology Initiative.

## References and Notes

- (1) Hassey, R.; Swain, E. J.; Hammer, N. I.; Venkataraman, D.; Barnes, M. D. *Science* **2006**, *314*, 1437.
- (2) Moerner, W. E.; Kador, L. *Phys. Rev. Lett.* **1989**, *62*, 2535.
- (3) Moerner, W. E. *Proc. Natl. Acad. Sci. U.S.A.* **2007**, *104*, 12596.
- (4) Selvin, P. R.; Ha, T. *Single Molecule Techniques: A Laboratory Manual*; Cold Spring Harbor Laboratory Press: New York, 2007.
- (5) Bauer, M.; Kador, L. *J. Chem. Phys.* **2004**, *120*, 10278.
- (6) Vainer, Y. G.; Naumov, A. V. *Opt. Spectrosc.* **2005**, *98*, 747.
- (7) Dickson, R. M.; Cubitt, A. B.; Tsien, R. Y.; Moerner, W. E. *Nature* **1997**, *388*, 355.
- (8) Le Floc'h, V.; Brasselet, S.; Roch, J. F.; Zyss, J. *J. Phys. Chem. B* **2003**, *107*, 12403.
- (9) Dickson, R. M.; Norris, D. J.; Moerner, W. E. *Phys. Rev. Lett.* **1998**, *81*, 5322.
- (10) Inoue, Y.; Ramamurthy, V. *Chiral Photochemistry (Molecular and Supramolecular Photochemistry)*; CRC Press: New York, 2004.
- (11) Schellman, J. A. *Chem. Rev.* **1975**, *75*, 323.
- (12) Barron, L. D. *Molecular Light Scattering and Optical Activity*; Cambridge University Press: Cambridge, U.K., 2004.
- (13) Craig, D. P.; Thirunamachandran, T. *Molecular Quantum Electrodynamics*; Dover Publications: New York, 1998.
- (14) Disch, R. L.; Sverdlik, D. I. *Anal. Chem.* **1969**, *41*, 82.
- (15) Tinoco Jr, I.; Turner, D. H. *J. Am. Chem. Soc.* **1976**, *98*, 6453.
- (16) Turner, D. H.; Tinoco Jr, I.; Maestre, M. *J. Am. Chem. Soc.* **1974**, *96*, 4340.
- (17) Tinoco Jr, I.; Ehrenberg, B.; Steinberg, I. *Z. J. Chem. Phys.* **1977**, *66*, 916.
- (18) Hassey, R.; McCarthy, K. D.; Swain, E.; Basak, D.; Venkataraman, D.; Barnes, M. D. *Chirality* **2008**, *20*, 1039.
- (19) Field, J. E.; Muller, G.; Riehl, J. P.; Venkataraman, D. *J. Am. Chem. Soc.* **2003**, *125*, 11808.
- (20) Field, J. E.; Hill, T. J.; Venkataraman, D.; He, H.; Janso, J. E.; Williamson, R. T.; Yang, H. Y.; Carter, G. T.; Carra, C.; Ghigo, G. *J. Org. Chem.* **2003**, *68*, 6071.
- (21) Driver, M. S.; Hartwig, J. F. *J. Am. Chem. Soc.* **1996**, *118*, 7217.
- (22) Ten equivalents of  $\text{BBr}_3$  (1.0 M in  $\text{CH}_2\text{Cl}_2$ ) were added to a solution of the helicene methyl ether in  $\text{CH}_2\text{Cl}_2$  at 0 °C. The reaction was stirred at 25 °C for 18 h, quenched with saturated aqueous  $\text{NaHCO}_3$ , and worked up as in ref 20. Yield was quantitative.
- (23) Schellman, J.; Jensen, H. P. *Chem. Rev.* **1987**, *87*, 1359.
- (24) Lakowicz, J. R. *Principles of Fluorescence Spectroscopy*; Springer Science: Singapore, 2006.
- (25) Claborn, K.; Puklin-Faucher, E.; Kurimoto, M.; Kaminsky, W.; Kahr, B. *J. Am. Chem. Soc.* **2003**, *125*, 14825.

JP903598T